

An Optically Powered Wireless Telemetry Module for High-Temperature MEMS Sensing and Communication

Michael Suster, *Member, IEEE*, Wen H. Ko, *Life Fellow, IEEE*, and Darrin J. Young, *Member, IEEE*

Abstract—A high-temperature, low-power silicon tunnel diode oscillator transmitter with an on-board optical power converter is proposed for harsh environment MEMS sensing and wireless data telemetry applications. The prototype sensing and transmitting module employs a MEMS silicon capacitive pressure sensor performing pressure to frequency conversion and a spiral loop serving as an inductor for the LC tank resonator and also as a transmitting antenna. A GaAs photodiode converts an incoming laser beam to an electrical energy for powering the prototype design. The system achieves a telemetry performance up to 250 °C over a distance of 1.5 m with a transmitter power consumption of approximately 60 μ W. [1042]

Index Terms—High-temperature, MEMS pressure sensor, remote powering, telemetry, wireless sensing.

I. INTRODUCTION

HIGH-TEMPERATURE, low-power wireless sensor communication network with on-board power supply is critical for industrial, automotive, and aerospace sensing and data telemetry applications. Typical temperatures for these applications range from 200 to 600 °C. Conventional microelectronics based on bipolar junction transistor (BJT) and complimentary metal–oxide–semiconductor (CMOS) technologies suffer from severe performance degradation and failure above 180 °C due to excessive leakage currents [1]. Silicon on insulator (SOI) [2] and silicon carbide (SiC) [3], [4] device technologies are promising for increased operating temperatures of 250 and 600 °C, respectively. However, SOI-based electronic telemetry systems would require a supply voltage of a few volts resulting in a significant power dissipation, which is undesirable for high-temperature applications where power source is highly limited. SiC device technology is still under development. Conventional battery technologies such as solid state lithium batteries suffer from severe performance degradation for temperatures above 150 °C, limited by electrochemical process constraints [5]. Miniature high-temperature battery is yet under development [6]. Thermoelectric generators have been proposed to convert temperature gradients in a high-temperature environment to a dc power [7]. However, this approach is only applicable for a limited temperature range and may require a complex wiring setup to ensure

proper temperature gradients. An RF to dc power conversion method has also been considered for remote powering applications [8]–[10]. This technique requires high-temperature electronics for voltage regulation and suffers from a limited coupling distance, which is undesirable for harsh environment applications.

Most of the conventional high-temperature sensing applications rely on using piezoresistive sensors made of silicon or silicon carbide material [11], [12]. These sensors, however, exhibit a strong temperature dependence and suffer from contact resistances variation at elevated temperatures. The devices also require feed-through wires for external power supply and signal detection, thus, severely limiting the system flexibility and performance. Capacitive sensors are attractive for high-temperature sensing due to their small temperature dependence and immunity to contact resistances. High-temperature capacitive sensing has been demonstrated by employing a resonant load sensing method [13]. This technique does not require any feed-through wires but suffers from a limited coupling distance of approximately one inch, which is undesirable for high-temperature applications. In this paper, a high-temperature stand alone capacitive sensing and wireless data telemetry module with an on-board optical-based power converter is presented. The prototype system eliminates any feed-through wires and achieves a telemetry distance of 1.5 m under operating temperatures up to 250 °C. The demonstrated performance is suitable for various high-temperature industrial sensing applications.

II. HIGH-TEMPERATURE SENSING AND TELEMETRY SYSTEM

Fig. 1 presents the high-temperature prototype architecture. The system consists of a silicon tunnel diode LC-tuned oscillator transmitter employing a MEMS capacitive pressure sensor with an on-board spiral loop inductor also functioning as a telemetry antenna and a GaAs photodiode, which converts an incoming laser to a dc power at high temperatures. The negative resistance characteristics exhibited by the tunnel diode under a proper bias condition can compensate the tank loss, thus ensuring a reliable oscillation over a large temperature range. The dc bias voltage required to properly bias the device typically ranges from 100 mV to 150 mV. This low bias voltage can be readily obtained from a GaAs photodiode, thus substantially simplifying the system implementation. The low bias voltage also significantly minimizes the oscillator power

Manuscript received April 17, 2003; revised October 15, 2003. This work was supported in part by NASA under the Glenn Microsystems Initiative. Subject Editor H. Fujita.

The authors are with the Electrical Engineering and Computer Science Department, Case Western Reserve University, Cleveland, OH 44106-7221 USA (e-mail: mas20@cwru.edu; djy@cwru.edu).

Digital Object Identifier 10.1109/JMEMS.2004.828706

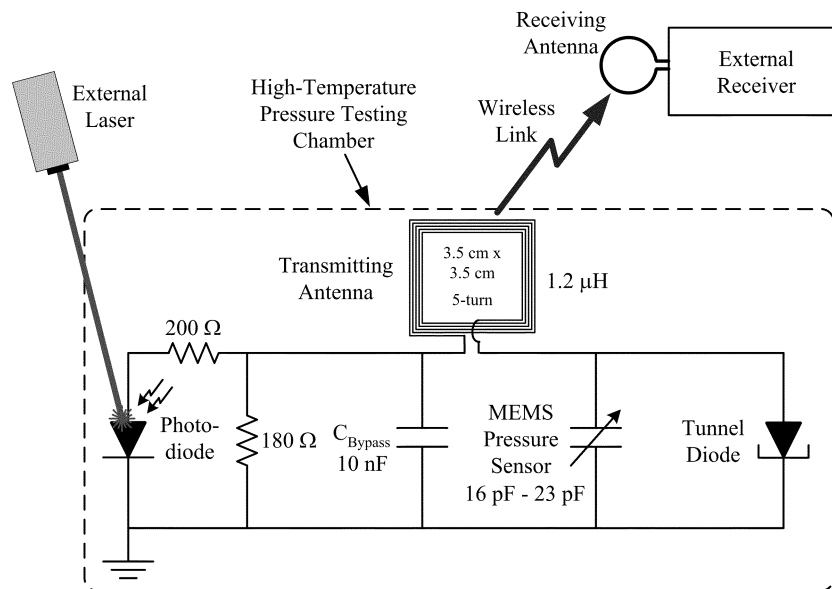


Fig. 1. High-temperature wireless sensing architecture.

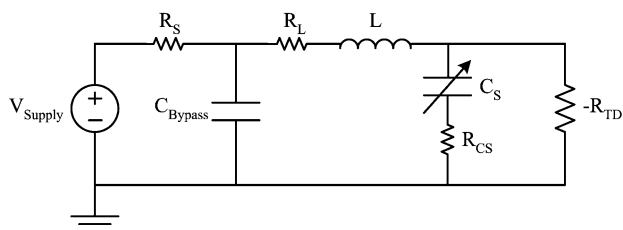


Fig. 2. Oscillator small-signal model.

dissipation, which is a key advantage over other high-temperature electronic oscillator designs requiring a supply voltage of a few volts. Fig. 2 shows a simplified electrical small-signal model for the proposed system, where $-R_{TD}$ is the negative resistance from the tunnel diode under a proper bias, C_S and R_{CS} are the capacitive pressure sensor capacitance and series resistance, respectively, and L and R_L represent the inductance and series resistance of the on-board spiral loop inductor, respectively. The bypass capacitor, C_{Bypass} , suppresses the loading effect from the supply voltage source resistance, R_S , at the operating frequency. Under the condition that R_{TD} is less than the total resistive loss contributed by the resonant network of L and C_S , an oscillation will be developed in the circuit with a steady-state frequency equal to the network resonance, $(2\pi\sqrt{LC_S})^{-1}$. The MEMS capacitive pressure sensor converts the environment pressure information to a capacitance change, thus resulting in an oscillator output frequency variation. This frequency change can be detected by an external receiver through the wireless link. The pressure to frequency modulation scheme is attractive for achieving a reliable data transmission compared to other amplitude modulation techniques. The GaAs photodiode converts the power of an incoming laser beam into a dc power supply for the prototype system, thus eliminating any feed-through wires. This is a critical advantage for realizing stand alone high-temperature wireless sensing and telemetry module. The GaAs photodiode is chosen for the prototype system due to its relatively large band gap, which

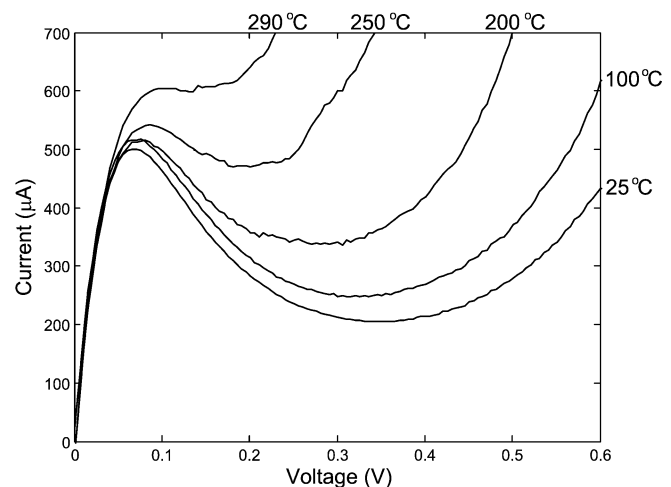


Fig. 3. Tunnel diode I - V curves at various temperatures.

is desirable for high-temperature applications. The proposed optical powering method is capable of achieving a much larger coupling distance than conventional RF to dc power conversion schemes and is attractive as an ON-OFF control to activate the system.

Fig. 3 shows the I - V characteristics measured at various temperatures for a silicon tunnel diode used for the prototype implementation. The diode has peak and valley currents ranging from $500 \mu\text{A}$ to $550 \mu\text{A}$ and $225 \mu\text{A}$ to $475 \mu\text{A}$ over a temperature range from 25 to 250°C , respectively. This results in a negative resistance of -500Ω for the bias condition of 160 mV and $340 \mu\text{A}$ at 25°C and -850Ω for 120 mV and $520 \mu\text{A}$ at 250°C , respectively. The oscillator thus dissipates a dc power of approximately $60 \mu\text{W}$ over the temperature range. An LC-tuned tank circuit can be properly designed so that the negative resistances from the diode are sufficient enough to compensate the resistive loss associated with the tank circuit, as will be illustrated in Section III. The rising current level of the tunnel diode is caused by the increasing diode forward bias current at elevated tempera-

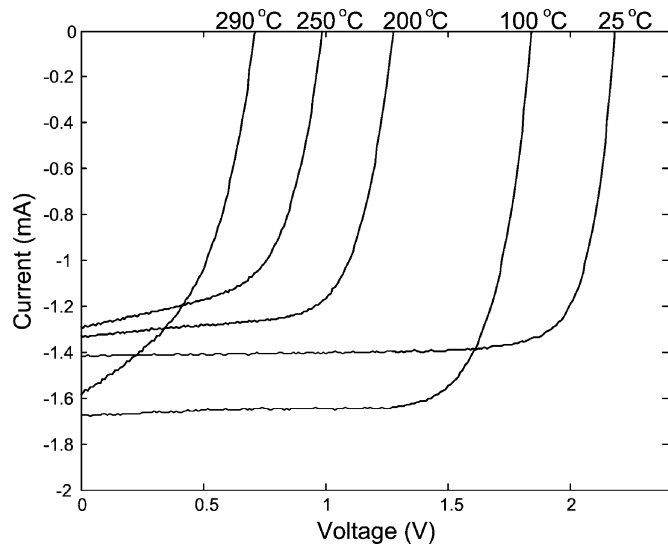


Fig. 4. Photodiode I - V curves at various temperatures.

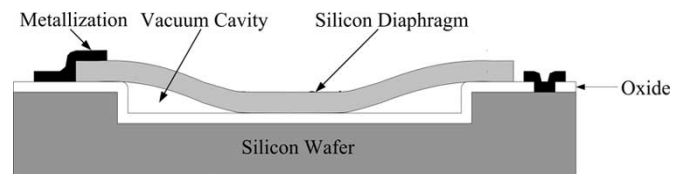


Fig. 5. Sensor cross-sectional view.

tures. From the measurement, a high-temperature operation up to 250 °C is expected for the prototype system. Fig. 4 shows the I - V characteristics of a 3 mm \times 4 mm GaAs photodiode measured over a temperature range from 25 to 290 °C with a laser beam of approximately 9 mW output power illuminating the surface. The photodiode area is chosen corresponding to the laser beam spot size. The device is capable of delivering a sufficient power for the prototype system with a conversion efficiency of 28% and 9% at 25 and 250 °C, respectively. A resistive bias network is implemented for the tunnel diode oscillator. As shown in Fig. 1, a bias network of two resistors with values of 200 Ω and 180 Ω are chosen to provide a proper dc bias voltage for the tunnel diode and also to ensure that the network output resistance is less than the absolute value of the maximum negative resistance from the tunnel diode over the large temperature range. This condition is critical for obtaining a stable oscillator operation [14]. The chosen resistors values also ensure that the photodiode is biased in a constant current region with a minimum temperature sensitivity and sufficient currents exceeding the tunnel diode peak current requirements.

A MEMS touch-mode silicon capacitive pressure sensor is employed as a demonstration vehicle for the prototype design. Fig. 5 presents a simplified cross-sectional view of the device. The sensor consists of an edge-clamped circular silicon diaphragm with a thickness of 5 μm and a radius of 400 μm over a vacuum cavity with a depth of 2.5 μm . The diaphragm deflects toward the substrate under an increasing external pressure, thus increasing the device capacitance value. Once the diaphragm touches the substrate at a designed touch point pressure, the sensor capacitance value increases linearly with the pressure due to the linearly increasing touched area.

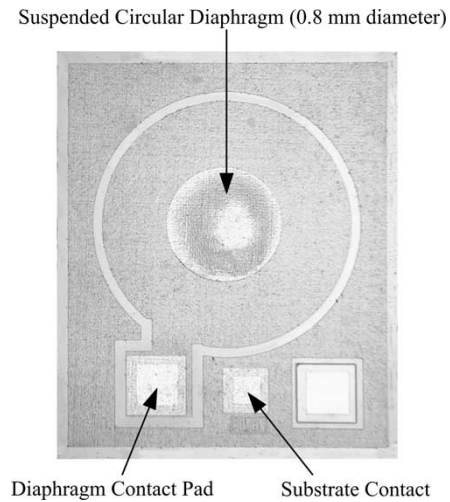


Fig. 6. MEMS pressure sensor top view.

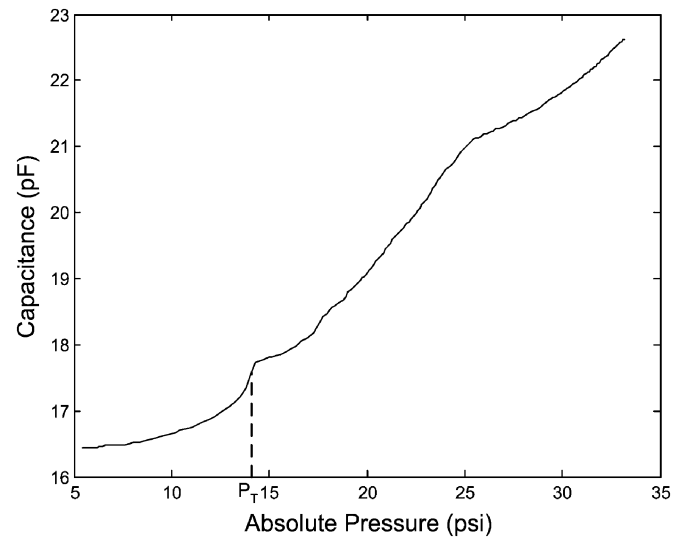


Fig. 7. MEMS pressure sensor characteristics.

The diaphragm thickness and radius and cavity depth can be designed to satisfy various pressure range and sensitivity requirements. The major device fabrication steps consist of 1) silicon substrate recess formation by reactive ion etch (RIE) followed by an oxidation process; 2) formation of a heavily-doped boron layer (p^+ layer) at the surface of a second silicon wafer through a diffusion process; 3) wafer bonding of the silicon substrate and the second wafer in vacuum followed by a high-temperature annealing step to strengthen the bonding quality; 4) removing the backside silicon substrate material from the second wafer through a TMAH wet etch followed by patterning the p^+ diaphragm using RIE; 5) opening contact windows and forming metal contacts. The detailed device design and fabrication process can be found in [15]. Fig. 6 shows a top view photograph of a fabricated pressure sensor consisting of a circular diaphragm with 800 μm diameter. The device exhibits a touch point pressure, P_T , of 14 psi and a capacitance value ranging from 16.4 pF at 5 psi to 22.6 pF at 33 psi (absolute pressure), as shown in Fig. 7. A linear characteristic behavior from 15 psi to 25 psi is obtained with

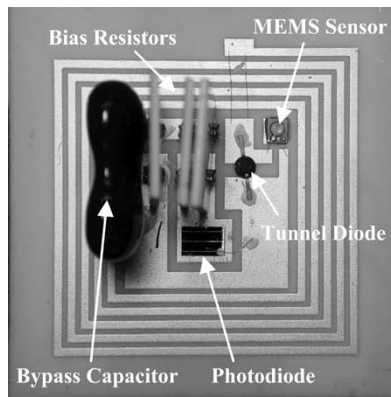


Fig. 8. Prototype board photograph.

a linearity of 1%. The sensor has a measured series resistance of 30Ω , which limits the oscillator operating frequency. A nominal frequency from an ISM band of 27 MHz is chosen for the prototype design, which results in a resonant network resistive loss of approximately $2.3 \text{ k}\Omega$ assuming the inductor contributes a negligible loss compared to the capacitive pressure sensor. This amount of loss thus can be adequately compensated by the tunnel diode negative resistance. With the sensor capacitance value and an estimated parasitic capacitance of 13 pF associated with the tunnel diode and setup, a 5-turn 3.5 cm by 3.5 cm spiral loop is designed to provide an inductance value of approximately $1.2 \mu\text{H}$ for the oscillation frequency [16]. The inductor winding traces have a cross section of $1 \text{ mm} \times 25 \mu\text{m}$ and are separated by 0.5 mm due to fabrication constraints. Gold material is used for implementing the traces to achieve a reliable inductor with a minimum series resistance of 3Ω , critical for ensuring a reliable oscillation start-up. Based on the capacitive pressure sensor performance illustrated in Fig. 7, the oscillator output frequency range can be determined from 24.4 MHz to 26.8 MHz. Increased operating frequencies can be obtained with redesigned low-loss capacitive sensors thus reducing the spiral inductor dimensions, which is attractive for further system miniaturization. Low-loss capacitive sensors and spiral inductors are also important for minimizing the required current level of the tunnel diode, resulting in a reduced power dissipation. Fig. 8 shows a photograph of the prototype wireless MEMS sensing and data telemetry system. The MEMS capacitive pressure sensor, tunnel diode, and photodiode are attached to the surface of a ceramic substrate by high-temperature-grade silver epoxy and gold-wire bonded to form the prototype system. High-temperature-grade resistors and capacitor are used for biasing and bypassing, thus ensuring a reliable high-temperature operation. A single layer of gold is used for implementing the interconnect and spiral inductor traces to simplify the fabrication process. All components are located at the center of the spiral loop for a compact design.

III. EXPERIMENT RESULTS

Fig. 9 shows the experiment setup for the prototype high-temperature wireless sensor communication module. The sensor telemetry system is positioned inside a pressure testing chamber with temperatures elevated and controlled through

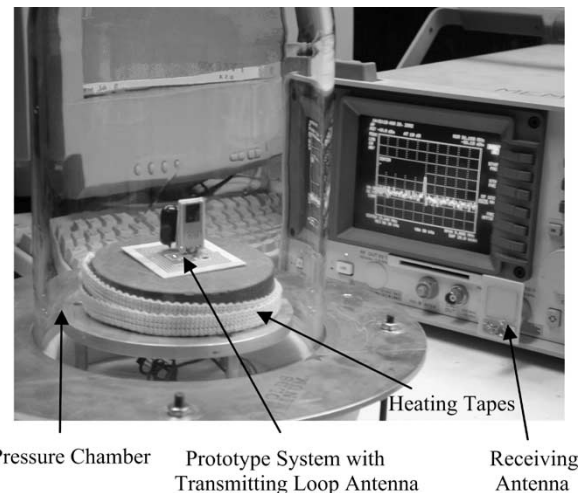


Fig. 9. Experiment setup.

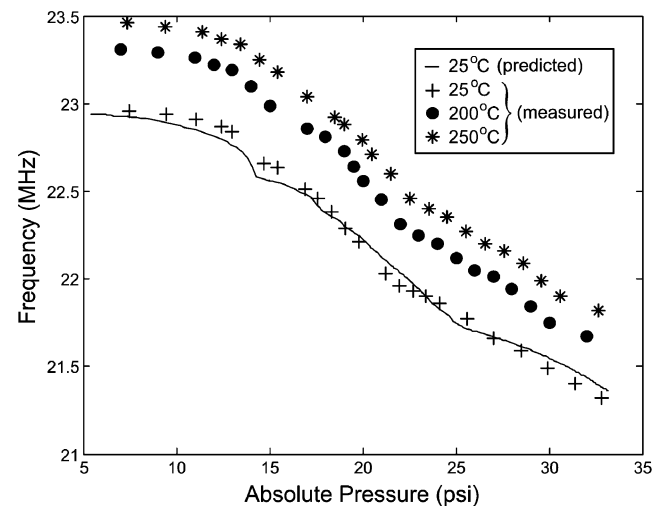


Fig. 10. Pressure versus frequency.

resistive heating tapes. An external laser source, not shown in the figure, is used to power the system. A spectrum analyzer is used as an external receiver with a tuned spiral loop connected to the input port through a buffer as a receiving antenna. The oscillator operates around 23 MHz under 1 atm at 250°C and can be varied over 1.7 MHz through a pressure increase from 7 psi to 32 psi (absolute pressure), as shown in Fig. 10. The reduced operating frequency and frequency variation range are caused by a larger parasitic capacitance of 24 pF than the originally estimated value. The measurement data shows a near linear characteristic behavior between 15 psi and 32 psi with a linearity of 0.5% and a sensitivity of 77 KHz per psi for all temperatures. Fig. 10 also presents the predicted system response at 25°C , shown by the solid-line curve, based on the sensor characteristic behavior and parasitic capacitance. The predicted response closely matches the experimental curve. The prototype oscillator exhibits a frequency reduction of 160 KHz when positioned from over a wood substrate to a ceramic heater substrate, which is caused by an increase in parasitic capacitance of the spiral inductor. Placing the oscillator over a metallic surface with a few millimeters air gap would result in

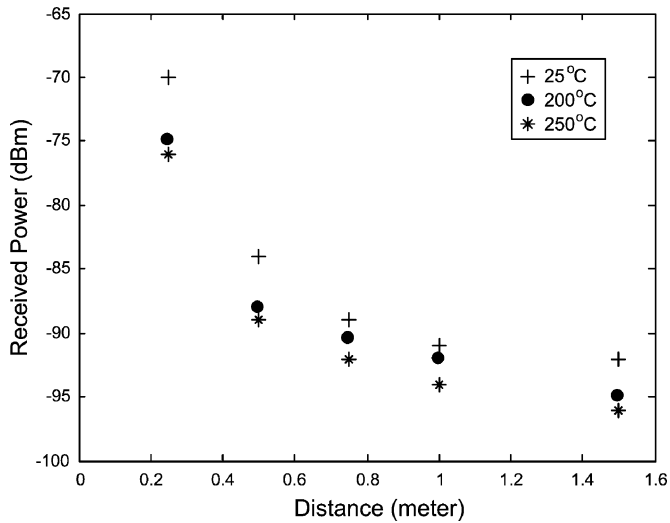


Fig. 11. Received power versus distance.

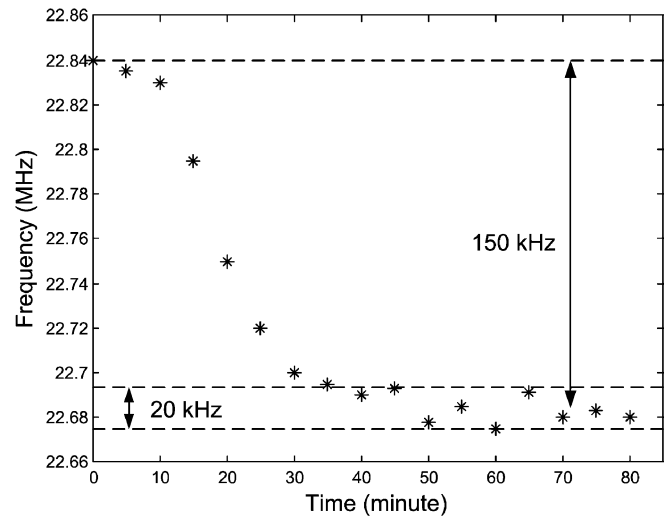


Fig. 13. Initial frequency drift versus time.

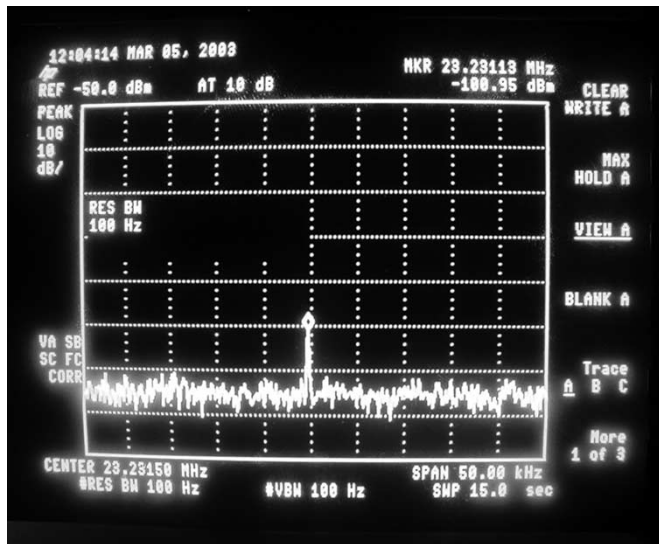


Fig. 12. Received power spectrum.

a spiral inductance drop from 1.2 to 0.98 μH due to the eddy current effect, causing a nominal oscillation frequency increase of approximately 2 MHz. These substrate effects, however, can be accurately measured and accounted in the system design process. The oscillator also exhibits a frequency shift of approximately 500 kHz over the temperature range from 25 to 250 $^{\circ}\text{C}$ due to the components temperature dependent characteristics and tunnel diode bias point shift. A temperature sensor thus will be required in a practical application to calibrate the system with a look-up table or a functional curve fit to minimize the thermal effect. An infrared-based temperature sensor can be readily implemented with the proposed system architecture for the calibration [17]. Fig. 11 presents the received power versus telemetry distance under 1 atm measured at 25, 200, and 250 $^{\circ}\text{C}$, respectively, indicating that the spectrum analyzer can receive an incoming signal over a telemetry distances of 1.5 m. Fig. 12 shows the corresponding received power spectrum at 1.5-m telemetry distance from the prototype oscillator operating at 250 $^{\circ}\text{C}$ with an SNR of 10 dB. The RF receiving

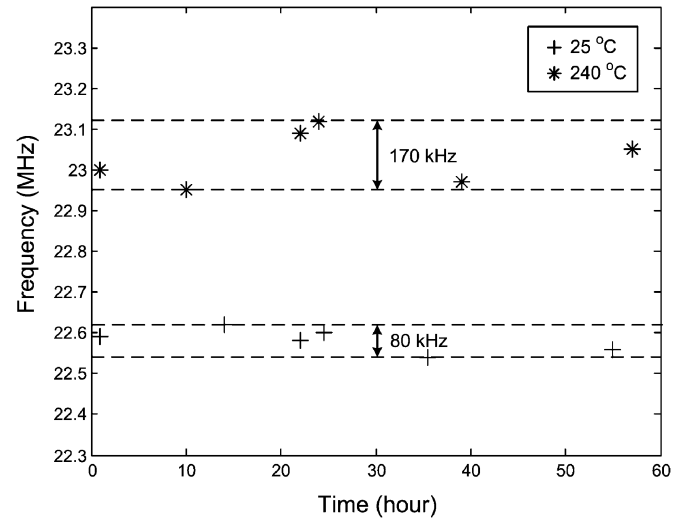


Fig. 14. Oscillator frequencies at fixed temperatures over time.

method does not affect the received frequency accuracy. However, the receiver noise floor limits the achievable telemetry distance. An extended communication range is thus expected with a more sensitive receiver. The prototype system exhibits an initial oscillation frequency turn-on decline of approximately 150 kHz over 30 min after it is activated at 250 $^{\circ}\text{C}$ as shown in Fig. 13. The system ultimately settles with a peak to peak frequency variation of 20 kHz, resulting in a sensing resolution of 0.13 psi (9 mbar). However, the oscillator measured over a three-day period shows a peak to peak frequency variation of 80 KHz and 170 KHz at 25 and 240 $^{\circ}\text{C}$, respectively, as presented in Fig. 14. The frequency drift can be possibly caused by the variations in the characteristic curves of the tunnel diode and photodiode due to temperature cycling and change in the laser output power. Fig. 15 shows the corresponding oscillator frequency versus pressure measurement data at 25 and 240 $^{\circ}\text{C}$ over a three-day period, indicating that the system can achieve a sensing repeatability of 0.5 psi (36 mbar) and 1.1 psi (76 mbar), respectively.

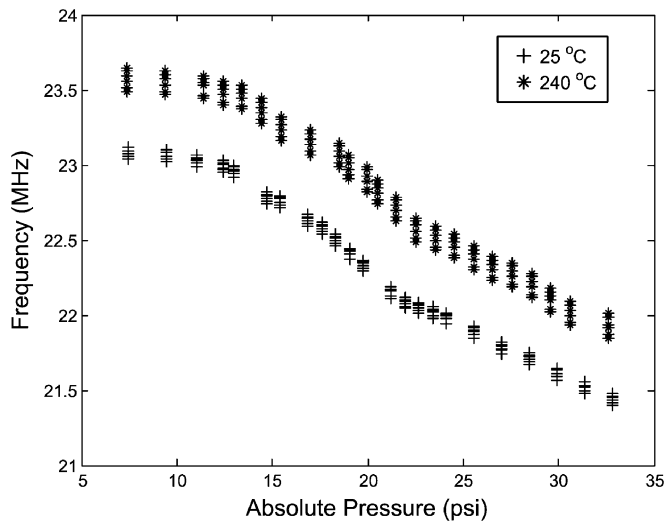


Fig. 15. Pressure versus frequency measured over time.

IV. CONCLUSION

Silicon tunnel diode oscillator transmitter with an on-board optical power converter is attractive for stand alone, high-temperature, and low-power MEMS sensing and data telemetry applications. The prototype wireless sensing and communication module achieves high-temperature operations up to 250 °C over a telemetry distance of 1.5 m. The demonstrated performance is suitable for various harsh environment industrial applications. The proposed architecture can also serve as a low-power platform for general wireless capacitive sensing and data telemetry applications.

REFERENCES

- [1] J. Goetz, "Sensors that can take the heat," *Sensors*, pp. 20–38, June 2000.
- [2] A. J. Auberton-Herve, "SOI: Materials to systems," in *Proc. International Electron Devices Meeting*, San Francisco, CA, Dec. 1996, pp. 3–10.
- [3] D. M. Brown, M. Ghezzi, J. Kretschmer, V. Krishnamurthy, G. Michon, and G. Gati, "High temperature silicon carbide planar IC technology and first monolithic SiC operation amplifier IC," in *Proc. Trans. 2nd International High-Temperature Elec. Conf. (HiTEC)*, 1994, pp. XI-17–XI-22.
- [4] P. G. Neudeck, R. S. Okojie, and L.-Y. Chen, "High temperature electronics—A role for wide bandgap semiconductors?," *Proc. IEEE*, vol. 90, pp. 1065–1076, June 2002.
- [5] J. B. Bates, G. R. Gruzalski, and C. F. Luck, "Rechargeable solid state lithium microbatteries," in *Proc. IEEE Micro Electro Mechanical Systems, MEMS '93*, Fort Lauderdale, FL, Feb. 1993, pp. 82–86.
- [6] D. Linden, *Handbook of Batteries*, 2nd ed. New York: McGraw-Hill, 1994.
- [7] T. Toriyama, M. Yajima, and S. Sugiyama, "Thermoelectric micro power generator utilizing self-standing polysilicon-metal thermopile," in *Proc. 14th IEEE International Conference on Micro Electro Mechanical Systems*, 2001, pp. 562–565.
- [8] S. Chatzandroulis, D. Tsoukalas, and P. A. Neukomm, "A miniature pressure system with a capacitive sensor and a passive telemetry link for use in implantable applications," *J. Microelectromech. Syst.*, vol. 9, pp. 18–23, Mar. 2000.
- [9] C. Hierold, B. Clasbrumme, D. Behrend, T. Scheiter, M. Steger, K. Oppermann, H. Kapels, E. Landgraf, D. Wenzel, and D. Etuodt, "Implantable low power integrated pressure sensor system for minimal invasive telemetric patient monitoring," in *Proc. IEEE Micro Electro Mechanical Systems, MEMS '98*, 1998, pp. 568–573.
- [10] K. Stangel, S. Kolnsberg, D. Hammerschmidt, B. J. Hosticka, H. K. Trieu, and W. Mokwa, "A programmable intraocular CMOS pressure sensor system implant," *IEEE J. Solid-State Circuits*, vol. 36, pp. 1094–1100, July 2001.

- [11] C.-H. Wu, S. Stefanescu, H.-I. Kuo, C. A. Zorman, and M. Mehregany, "Fabrication and testing of single crystalline 3C-SiC piezoresistive pressure sensors," in *Proc. 11th International Conference on Solid State Sensors and Actuators*, Munich, Germany, June 2001, pp. 514–517.
- [12] R. S. Okojie, A. A. Ned, A. D. Kurtz, and W. N. Carr, " α (6H)-SiC pressure sensors for high temperature applications," in *Proc. IEEE Micro Electro Mechanical Systems, MEMS '96*, San Diego, CA, Feb. 1996, pp. 146–149.
- [13] M. A. Fonseca, J. M. English, M. von Arx, and M. G. Allen, "Wireless micromachined ceramic pressure sensor for high-temperature applications," *J. Microelectromech. Syst.*, vol. 11, pp. 337–343, Aug. 2002.
- [14] W. F. Chow, *Principles of Tunnel Diode Circuits*. New York: Wiley, 1964.
- [15] W. H. Ko and Q. Wang, "Touch mode capacitive pressure sensors," *Sens. Actuators*, vol. 75, pp. 242–251, 1999.
- [16] T. H. Lee, *The Design of CMOS Radio-Frequency Integrated Circuits*. New York: Cambridge University Press, 1998.
- [17] W. R. Barron, "Principles of infrared thermometry," *Sensors*, pp. 20–29, Dec. 1992.



Michael Suster (M'03) received the B.S. and M.S. degrees in electrical engineering from Case Western Reserve University (CWRU), Cleveland, OH, in 2002 and 2004, respectively. He is currently pursuing the Ph.D. degree in electrical engineering at CWRU.

His current research interests include low-noise analog integrated circuit design for MEMS sensing applications.



Wen H. Ko (S'55–M'59–SM'75–F'78–LF'90) received the B.S.E.E. degree from Xiamen University of China in 1946 and the M.S. and Ph.D. degrees in electrical engineering from Case Institute of Technology, Cleveland, OH, in 1956 and 1959, respectively.

He has been a Faculty Member of Electrical Engineering and Biomedical Engineering Departments at Case Western Reserve University (CWRU), Cleveland, from 1959 to 1993. He became a Professor Emeritus in Electrical Engineering at CWRU in July 1993. He has 21 patents and 317 publications, with 131 in referenced journals, in areas of: solid-state electronics, microsensors and actuators, biomedical instrumentation, implant electronics, and control system design.

Dr. Ko is a Fellow of the American Institute of Medical and Biological Engineering. He is on the editorial board of *Sensors and Actuator*, *Micro-system Technologies*, *Telemetry and Patient Monitoring* (1974–1984), and *Medical Progress Through Technology* (1983–1988). He was the Chairman of International Steering Committee on Solid-State Sensors and Actuators conferences from 1983 to 1987 and the Chairman of the International Steering Committee on Chemical Sensor meetings from 1991 to 1993. He received the Career Achievement Award in the Transducer'97 Conference, Chicago, IL. He has been the President of the Transducer Research Foundation that sponsored the Hilton Head Workshops on Sensors and Actuators, Hilton Head, SC, since 1992.



Darrin J. Young (S'92–M'99) received the B.S., M.S., and Ph.D. degrees from the Department of Electrical Engineering and Computer Sciences at University of California at Berkeley in 1991, 1993, and 1999, respectively.

He joined the Department of Electrical Engineering and Computer Science at Case Western Reserve University (CWRU), Cleveland, OH, as an Assistant Professor in 1999. His research interests include MEMS design and fabrication, and integrated analog circuits design for wireless communications, sensing, biomedical implant, and general industrial applications.